

SUPPLEMENTARY MATERIALS

Li-rich strategy towards advanced Mn-doped triphylite cathodes for Li-ion batteries

Eugene E. Nazarov¹, Artem D. Dembitskiy¹, Ivan A. Trussov¹, Oleg A. Tyablikov¹, Iana S. Glazkova², Sobolev V. Alexey², Igor A. Presniakov², Ivan V. Mikheev², Anatolii V. Morozov^{1,2}, Victoria A. Nikitina¹, Artem M. Abakumov¹, Evgeny V. Antipov^{1,2}, Stanislav S. Fedotov¹

¹ Skoltech Center for Energy Science and Technology, Skolkovo Institute of Science and Technology, Nobel str. 3, 121205 Moscow, Russian Federation

² Department of Chemistry, Lomonosov Moscow State University, 119991 Moscow, Russian Federation

Table S1. Elemental composition determined by means of ICP-OES.

Element	Concentration, atomic units	Resulting chemical formula
Fe	0.49(3)	$\text{Li}_{1.00(6)}\text{Fe}_{0.49(3)}\text{Mn}_{0.49(3)}\text{P}_{1.00(6)}\text{O}_4$
Mn	0.49(3)	
P	1.00(6)	
Li	1.00(6)	

Speaking of precision variability between different emission lines of lithium would be a spectroscopic issue (e.g., due to the interference). For analysis, a set of three lithium atomic lines at 460.289(I), 610.365(I), and 670.783(I) nm was chosen. However, 610.365(I) and 670.783(I) nm possessed more significant interference with Ar-lines, the main plasma component. The best accuracy and reproducibility was observed at 460.289(I). Another reason for the increase in determination error is the high sample dilution, which cannot be avoided because of the limited linear range of lithium determination. Taking into account the above-mentioned features, it is impossible to precisely resolve the exact lithium concentration and the obtained data were used as preliminary model for structure refinement.

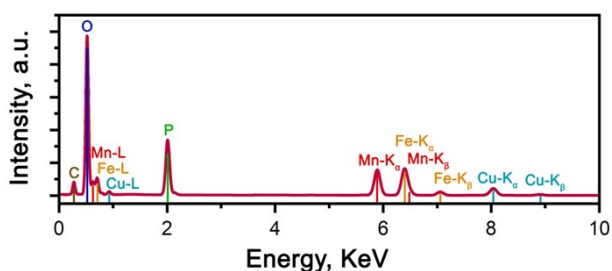


Fig.S1 Typical EDX spectrum of Li-rich LFMP.

Table S2. Cationic composition of $\text{Li}_{1+\delta}(\text{Fe}_{0.5}\text{Mn}_{0.5})_{1-\delta}\text{PO}_4$ calculated from the TEM-EDX data.

	Atomic fraction, at. % (calculated from K-lines)	
	Fe	Mn
Spectrum 1	51.71	48.29
Spectrum 2	50.9	49.1
Spectrum 3	50.36	49.64
Spectrum 4	51.94	48.06
Spectrum 5	50.92	49.08
Average	51.17	48.83
Standard deviation	0.65	0.65

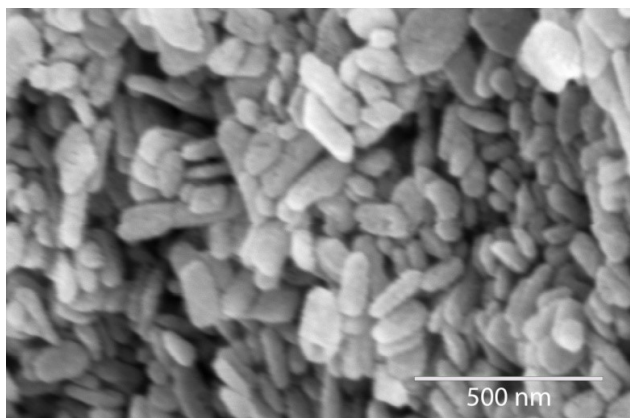


Figure S2. SEM image of the as-prepared material.

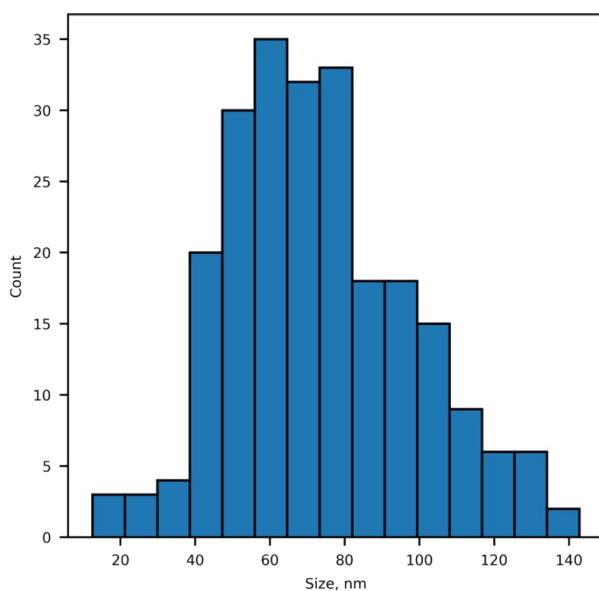


Figure S3. Particle size distribution of Li-rich LFMP.

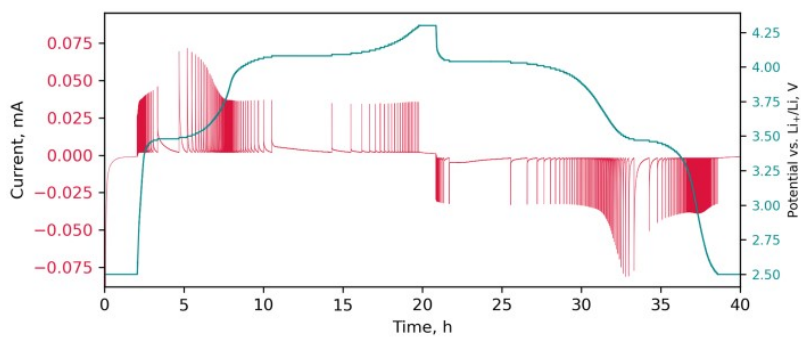


Figure S4. PITT experimental data.

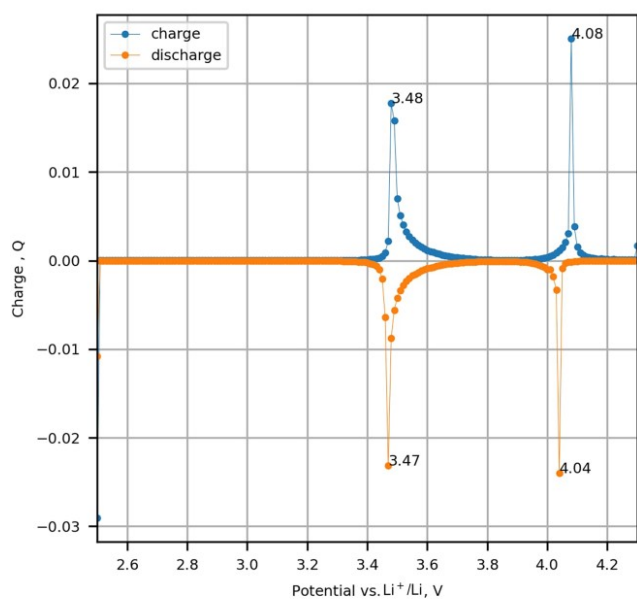


Figure S5. Incremental charge extracted from PITT experiment.

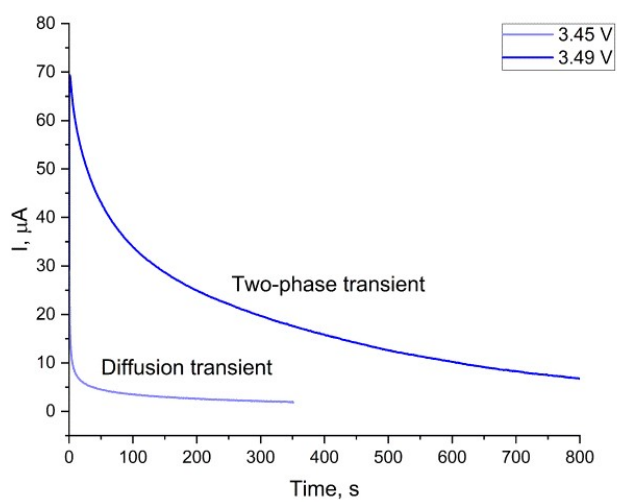


Figure S6. Current transients of PITT experiment.

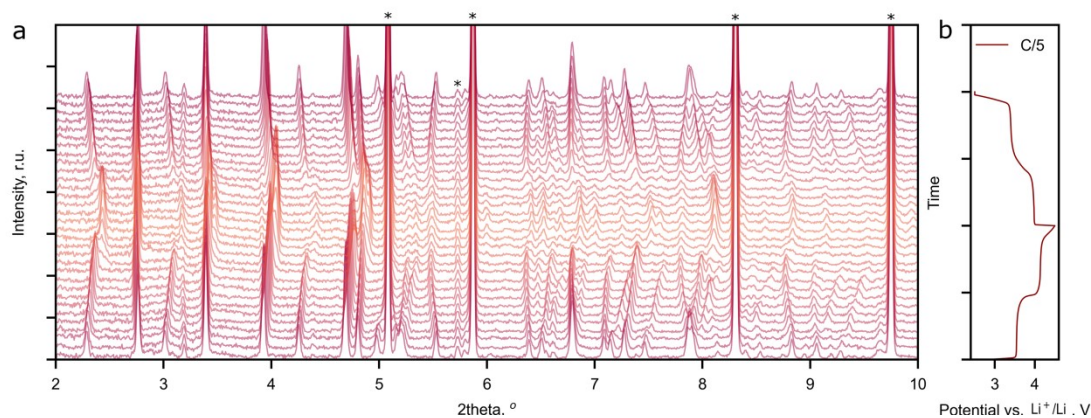


Figure S7. a) Waterfall plot of diffraction patterns obtained from SXR *operando* study of Li-rich LFMP after background subtraction.* - labeled peaks are assigned to the cell parts. b) charge-discharge profile of Li-rich LFMP during the experiment.

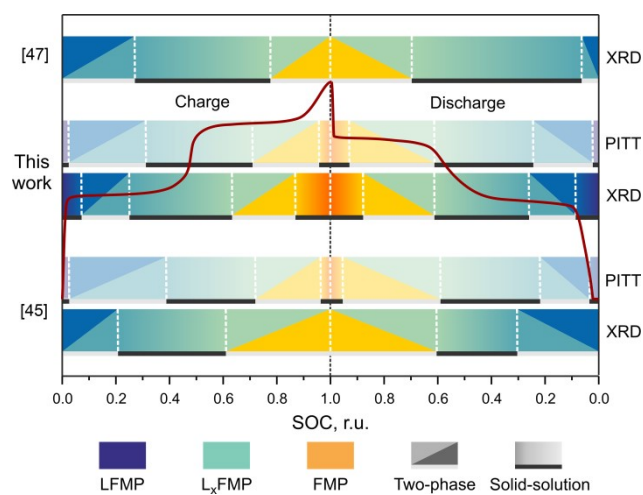


Figure S8. The comparison of de/intercalation mechanism of LFMP with the published data and the current work extracted from diffraction and electrochemical experiments.

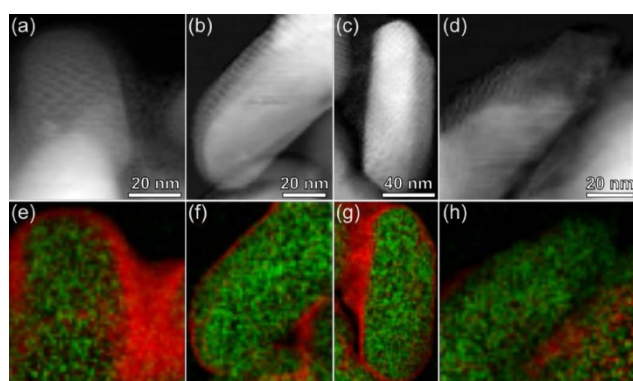


Figure S9. HAADF-STEM images (a-d) of Li-rich LFMP/C and corresponding STEM-EELS maps (e-h) of C (red) and Mn (green).